

## Rotational tunneling in solids: The theory of neutron scattering

Alfred Hüller

*Institut für Festkörperforschung der Kernforschungsanlage Jülich 5170 Jülich, West Germany  
and Institut für Physik der Universität Dortmund, 4600 Dortmund, West Germany*

(Received 23 February 1977; revised manuscript received 2 May 1977)

The wave functions of tunneling four proton groups (e.g.,  $\text{CH}_4$ ,  $\text{NH}_4^+$ ) in a crystal field of low symmetry are obtained from products of pocket states and proton spin states. The results are applied to  $\text{CH}_4$  in phase II of solid methane, and to  $\text{NH}_4^+$  in  $(\text{NH}_4^+)_2\text{SnCl}_6^{--}$  and in  $(\text{NH}_4^+)\text{ClO}_4^-$ , where the tunneling spectra are known. It is shown that the observed degeneracy of two  $T$  levels in ammonium perchlorate is accidental. Neutron scattering can only supply an upper bound of 25 MHz for the difference of the two levels. It is suggested to enlarge the splitting by hydrostatic pressure or to determine its value at zero pressure by NMR techniques. The theory of neutron scattering from tunneling molecules is developed on the basis of the pocket-state formalism. Symmetry correlates the nuclear spin state and the rotational part of the wave functions in the tunneling levels. Therefore, the scattering from the four protons of one molecule is coherent, in contrast with the usual spin incoherence in protonated samples. Predictions about the angular and radial dependence of the scattering are made and experiments to examine these predictions are suggested. Angular averages of the cross section agree very well with the existing data.

### I. INTRODUCTION

The tunneling of molecules between different equilibrium orientations in the crystal field has been known for many years. Until a few years ago only integral information on the tunneling levels was available. Such information is contained in low-temperature specific-heat anomalies<sup>1-3</sup> or in NMR lines which, in the presence of rotational tunneling, remain narrow down to the lowest temperatures.<sup>4-10</sup>

Only recently it has become possible to detect transitions between individual tunneling states by sophisticated NMR techniques<sup>11-13</sup> and by phonon spectroscopy.<sup>14</sup> Also in triple-axis neutron spectroscopy, where the energy resolution has been pushed to 25  $\mu\text{eV}$ , direct observation of tunneling transitions has become possible.<sup>15</sup> The neutron back scattering method, with a resolution of 0.3  $\mu\text{eV}$ , nowadays overlaps with the NMR range. It has been successfully applied to the determination of complicated energy-level schemes.<sup>16-21</sup>

Neutron scattering investigations exist for the tunneling states of methyl groups,<sup>16</sup> of methane molecules,<sup>15</sup> and of ammonium ions in various environments.<sup>18,21</sup> For tetrahedral molecules with heavy nuclei at the corners (e.g.,  $\text{CCl}_4$ ) the tunnel splitting is much too small to be observed by neutron scattering techniques. For  $\text{CD}_4$  an experiment is feasible and the transition frequencies have been estimated,<sup>22</sup> but the complexity of the low-temperature structure will be reflected in the tunneling pattern. Heavy methane will not be treated in this paper, but an extension of the method to  $\text{CD}_4$  is straightforward.

In the following the theory of neutron scattering

from the tunneling states of tetrahedrally coordinated  $\text{H}_4$  groups ( $\text{CH}_4$ ,  $\text{NH}_4^+$ ) will be developed. The intention is to find the energy levels and the correctly symmetrized wave functions of the librational ground-state multiplet. Once the wave functions are known it is easy to calculate the double differential neutron scattering cross section:

$$\frac{d^2\sigma}{d\Omega d\omega} = \frac{k'}{k} \sum_{\mu\mu'} \sum_{\alpha\alpha'} P_\mu P_\alpha |\langle \Psi_{\alpha'} | \langle \mu' \vec{k}' | W | \mu \vec{k} \rangle | \Psi_\alpha \rangle|^2 \times \delta(\omega - \omega_{\alpha, \alpha'}). \quad (1.1)$$

Unprimed symbols relate to quantities before the scattering event, primed symbols to the same quantities after scattering.  $\Omega$  denotes the solid angle and  $\hbar\omega$  the transferred energy.  $|\mu \vec{k}\rangle$  is a plane-wave state of the neutron:  $|\mu\rangle e^{i\vec{k}\cdot\vec{r}}$ , where  $|\mu\rangle$  denotes the spin state of the neutron which may either be up  $|\mu\rangle = |\alpha\rangle$  or down  $|\mu\rangle = |\beta\rangle$ .  $|\Psi_\alpha\rangle$  is the state of the scatterer,  $P_\mu$  and  $P_\alpha$  denote the initial probabilities for the neutron spin state and for the state of the scattering system.  $\hbar\omega_{\alpha, \alpha'}$  is the energy difference  $E_\alpha - E_{\alpha'}$  between the states  $|\Psi_\alpha\rangle$  and  $|\Psi_{\alpha'}\rangle$ .  $W$  is the interaction between the neutron and the scatterer:

$$W = \sum_{n=1}^N \sum_{\gamma=1}^4 A^{n\gamma} \delta(\vec{r} - \vec{R}_{n\gamma}), \quad (1.2)$$

$$A^{n\gamma} = a_{\text{coh}} + \{2a_{\text{inc}}/[I(I+1)]^{1/2}\} \vec{S} \cdot \vec{I}_{n\gamma}. \quad (1.3)$$

$\vec{R}_{n\gamma}$  is the position of the  $\gamma$ th proton in the  $n$ th molecule,  $\vec{I}_{n\gamma}$  is its spin operator. Equivalently the index pair  $n\gamma$  may define the  $4N$  sites in the crystal which are occupied by protons.  $\vec{R}_{n\gamma}$  and  $\vec{I}_{n\gamma}$  then are position and spin operators of the proton at the site  $n\gamma$  without identifying which one of the four protons of the  $n$ th molecule is concerned.

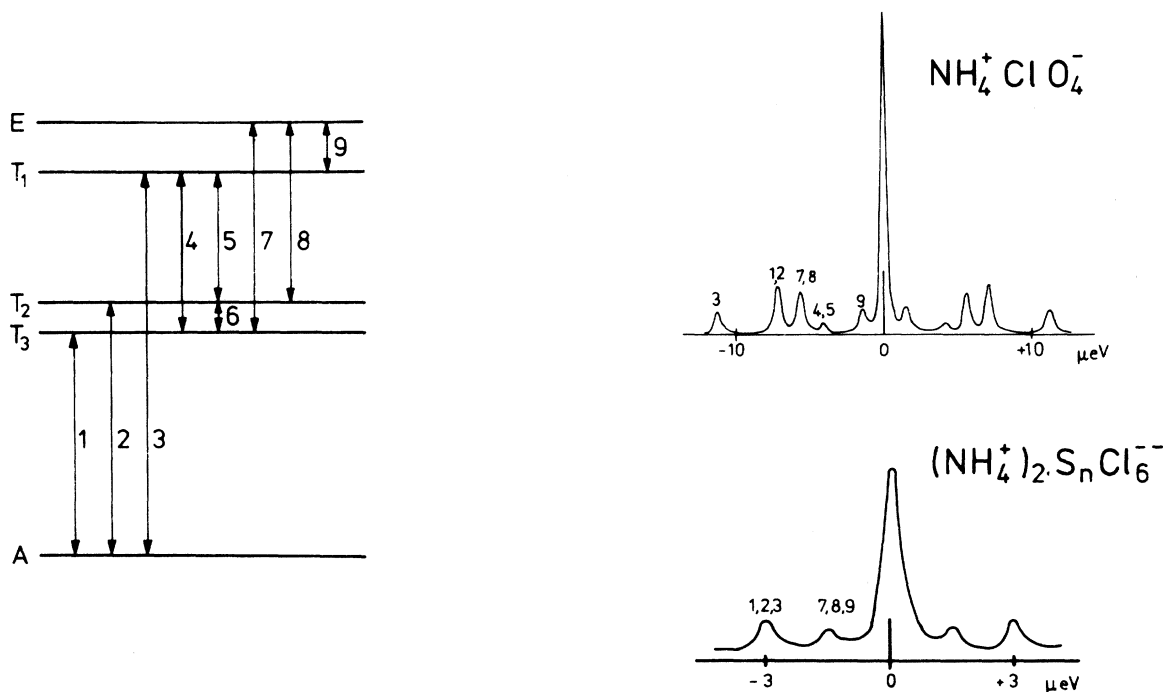


FIG. 1. General case of the energy levels of a regular tetrahedron in a field which has no symmetry. Also shown are the neutron scattering intensities for  $\text{NH}_4^+\text{ClO}_4^-$  (Refs. 17 and 18) and  $(\text{NH}_4^+)_2\text{SnCl}_6^{--}$  (Ref. 21) as functions of the energy transfer. The spectrum of  $\text{CH}_4$  in phase II of solid methane (Ref. 15) is similar to the one of  $(\text{NH}_4^+)_2\text{SnCl}_6^{--}$ , but the lines appear at much higher energies (143 and 73  $\mu\text{eV}$ ).

$\vec{S}$  is the spin operator of the neutron,  $\vec{r}$  its position. The spin-independent part of the proton scattering length is denoted by  $a_{\text{coh}}$ , the spin-dependent part by  $a_{\text{inc}}$ . Because of the extremely small energy transfer in tunneling spectroscopy  $k$  and  $k'$  are almost equal and the factor  $k'/k$  can be omitted.

In Sec. II it will be shown, that the tunneling between equivalent orientations is of an extreme single-particle character. The states  $|\Psi_\alpha\rangle$  of the system of tunneling molecules thus are products of single molecule states  $|\psi_\alpha\rangle$ . Section III is devoted to the construction of the states  $|\psi_\alpha\rangle$  and to

the determination of the corresponding energy levels  $E_\alpha$  in terms of overlap matrix elements. Explicit calculations are performed for a tetrahedron in a tetrahedral crystal field [ $(\text{NH}_4^+)_2\text{SnCl}_6^{--}$ , approximate symmetry also for  $\text{CH}_4$  in phase II] and for a tetrahedron at a site with a mirror plane as the only symmetry element ( $\text{NH}_4^+\text{ClO}_4^-$ ). An impression of the experimental situation may be obtained from Fig. 1 and Table I. The degeneracy of all three  $T$  levels in  $(\text{NH}_4^+)_2\text{SnCl}_6^{--}$  is due to symmetry, the degeneracy of  $T_2$  and  $T_3$  in  $\text{NH}_4^+\text{ClO}_4^-$  is accidental.

With the knowledge of the tunneling wave func-

TABLE I. Energies and intensities of the tunneling transitions in  $\text{NH}_4^+\text{ClO}_4^-$  (Ref. 18) and  $(\text{NH}_4^+)_2\text{SnCl}_6^{--}$  (Ref. 21) with different arbitrary units for the two experiments. The experimental intensities are compared with the theoretical scattering cross section {in units of  $\frac{1}{24} N a_{\text{inc}}^2 [1 - f(x)]$ } which are calculated in Sec. IV.

	$\text{NH}_4^+\text{ClO}_4^-$					$(\text{NH}_4^+)_2\text{SnCl}_6^{--}$	
Line	1, 2	3	4, 5	7, 8	9	1, 2, 3	7, 8, 9
$\hbar\omega$ ( $\mu\text{eV}$ )	7.17	11.28	4.11	5.65	1.51	3.0	1.5
Intensity (arb. units)	104	49	22	84	50	35	26
$\sigma$	10	5	2	8	4	15	12

tions, Eq. (1.1) for the neutron scattering cross section can be evaluated. This is done in Sec. IV. Symmetry requirements relate the nuclear-spin states and the rotational wave functions in the tunneling levels and therefore the four protons within one molecule scatter the neutrons coherently. The angular and radial dependence of the scattering intensity is predicted and single-crystal experiments, to test these predictions, are suggested. Polycrystalline averages of the intensities are compared with the existing experimental results.

## II. SINGLE-PARTICLE POTENTIAL

The rotational motion of the methane molecules or ammonium ions in the crystal is governed by the Hamiltonian

$$\mathcal{H}_0 = \sum_{n=1}^N T_n + V_0(\omega_1, \omega_2, \dots, \omega_N), \quad (2.1)$$

where  $T_n$  is the rotational kinetic energy of the  $n$ th tetrahedron, and  $V_0(\omega_1, \omega_2, \dots, \omega_N)$  is the rotational energy which depends on suitable orientational coordinates  $\omega_n$  (Euler angles, quaternions, etc.).  $V_0$  is a sum of single-particle potentials and of two-particle interactions:

$$V_0 = \sum_{n=1}^N V_n(\omega_n) + \sum_{\langle n, m \rangle} V_{nm}(\omega_n, \omega_m). \quad (2.2)$$

The symbol  $\langle n, m \rangle$  denotes a sum over pairs of molecules (to avoid double counting).

$V_0$  thus consists of terms which depend on the orientation of both units (as, e.g., the octopole-octopole interaction) and of terms which depend only on the orientation of one of the partners (as, e.g., a monopole-octopole interaction). In ionic crystals as  $\text{NH}_4^+\text{ClO}_4^-$  or  $(\text{NH}_4^+)_2\text{SnCl}_6^{2-}$  the main contribution to  $V_n(\omega_n)$  stems from the interaction of a tetrahedron with the static (not reorienting) ions in its surrounding.

The Hartree potential for one of the tetrahedra is given by

$$V_n^{(H)} = V_n(\omega_n) + \sum_m \int d\omega_m \rho_m(\omega_m, \omega_m) V_{nm}(\omega_n, \omega_m). \quad (2.3)$$

Here the rotational density matrix has been replaced by a product of single-particle density matrices  $\rho_m(\omega_m, \omega'_m)$ :

$$V_n^{(H)} = \sum_n V_n^{(H)}(\omega_n) \quad (2.4)$$

is a good approximation for  $V_0$ , if orientational correlations between adjacent tetrahedra are small. The eigenstates of a tetrahedron in the potential  $V_n^{(H)}(\omega_n)$  are the librational states which are split by the overlap between equivalent equi-

librium orientations. At low temperatures only the librational ground-state multiplet is occupied and therefore contributions of excited states to  $\rho_m(\omega_m, \omega'_m)$  are negligible.

The wave functions  $|\psi_\alpha\rangle$  of the ground-state multiplet will be calculated in the next paragraph. They are linear combinations of<sup>22</sup> pocket states  $|\varphi_i\rangle$ :

$$|\psi_\alpha\rangle = \sum_i a_{\alpha i} |\varphi_i\rangle. \quad (2.5)$$

The pocket states  $|\varphi_i\rangle$  differ from each other only by permutations of the four corners of a tetrahedron. Into (2.3) we insert

$$\rho(\omega_m, \omega'_m) = \sum_\alpha w_{m\alpha} \langle \omega_m | \psi_\alpha \rangle \langle \psi_\alpha | \omega'_m \rangle, \quad (2.6)$$

with  $w_{m\alpha} = e^{-\beta E_{m\alpha}} / \sum_{\alpha'} e^{-\beta E_{m\alpha'}}$ . All diagonal contributions  $V_{nm}(\omega_n, \omega_m) \langle \omega_m | \varphi_i \rangle \langle \varphi_i | \omega_m \rangle$  to (2.3) are identical. Off-diagonal terms  $V_{nm}(\omega_n, \omega_m) \langle \omega_m | \varphi_i \rangle \langle \varphi_j | \omega_m \rangle$  are tiny if the pocket states are narrow. Consequently  $\rho_n(\omega_n, \omega_n)$  depends only very weakly on the occupations  $w_{n\alpha}$  and  $V_n^{(H)}(\omega_n)$  thus is nearly independent of the state of its neighbors. Consequently Eq. (2.4) turns out to be an excellent approximation for  $V_0(\omega_1, \omega_2, \dots, \omega_N)$ . It also shows that correlations between adjacent tetrahedra cannot develop. It thus has been established that the problem of tunneling between equivalent orientations is of an extreme single particle character.

## III. CONSTRUCTION OF THE PROPERLY SYMMETRIZED WAVE FUNCTIONS

In the following the  $\text{CH}_4$  or  $\text{NH}_4^+$  tetrahedra will be treated as rigid units. The consequences of this idealization are twofold: (i) the internal vibrations of the molecules are neglected which seems to be well justified considering the extreme smallness of the excitation energies that are observed in tunneling experiments. (ii) The other consequence is a neglect of the symmetry operations which change the molecular framework<sup>23</sup> (from right handed into left handed). Symmetry requirements of the wave function under the 12 even permutations of four identical particles (protons) are taken into account. These permutations correspond to proper rotations of the molecules, and they do not change the framework. The 12 odd permutations of the four protons are neglected as they do change the framework. One therefore obtains only half the states, e.g., all those of the right-handed molecules. The allowed wave functions have to be totally symmetric under the even permutations of the four protons (even number of proton exchange operations).

Translational motions of the molecules are also

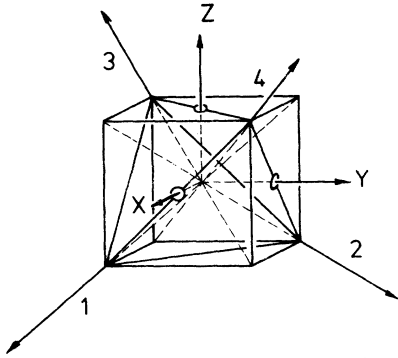


FIG. 2. Equilibrium position of a tetrahedron in the crystal field.  $180^\circ$  rotations around the X, Y, and Z axes, as well as  $120^\circ$  rotations around the 1-4 axes are symmetry operations of the tetrahedron. The rotation axes are all fixed in the crystal. In  $\text{NH}_4^+\text{ClO}_4^-$  the plane spanned by axes 1 and 2 is a mirror plane of the crystal. Rotation axes 3 and 4 as well as X and Y then are equivalent.

neglected. With the restriction to rotational motions only, the total wave function depends on the rotational coordinates and on the spin coordinates of the four protons.

#### A. Rotational wave function

To construct the rotational wave function of a molecule in the crystal one starts from an angular potential  $V^{(H)}$  that depends on suitable rotational coordinates as, e.g., the Euler angles<sup>24</sup> or the quaternions.<sup>22,25</sup> Let us rotate the crystal such that Figure 2 represents an equilibrium orientation of the molecule in the potential  $V^{(H)}$ . No assumptions will be made about the site symmetry at the molecular position. This may be expressed differently: One considers the most general case of the potential where the surrounding of the tetrahedron does not have any symmetry. The potential  $V^{(H)}$  nevertheless reflects the symmetry of the tetrahedron itself. In particular the 12 orientations shown in Fig. 3 are all equivalent and they are *all* equilibrium orientations if one of them is an equilibrium orientation. For sufficiently strong  $V^{(H)}$  the molecule performs small angular oscillations around one of these equilibrium orientations. Only the librational ground states in the 12 pockets of the potential are of importance in this context and they will be called the pocket states  $|\varphi_i\rangle$ . (The energies of the excited librational states are very large in comparison with tunneling frequencies.) The index  $i = 1, 2, \dots, 12$  denotes the corresponding

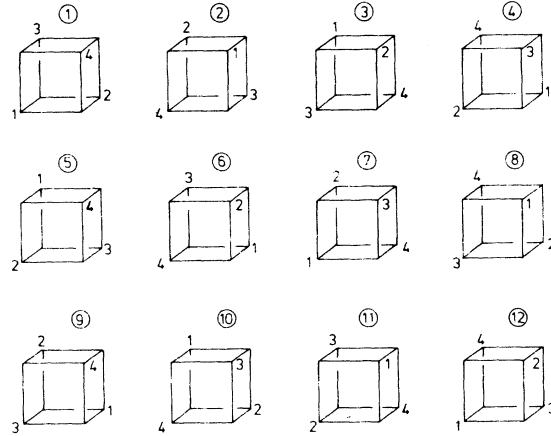


FIG. 3. If the first one of these orientations is an equilibrium orientation of the tetrahedron in the crystal field, then all 12 orientations are equilibrium orientations, irrespective of the symmetry of the crystal field. The 12 pocket states are the librational ground-state wave functions which are centered around these 12 distinct orientations.

equilibrium orientation as drawn in Fig. 3. The pocket states are no eigenstates of the system. Pocket states will oscillate in time because of the tunneling matrix elements between them.

The Hamiltonian  $\mathcal{H} = T + V^{(H)}$  of the tetrahedron therefore is not diagonal in the subspace of the pocket states ( $T$  is the rotational kinetic energy). The diagonal elements  $\mathcal{H}_{ii} = D$  are all equal. There are seven different off-diagonal matrix elements of  $\mathcal{H}$ .  $\mathcal{H}_{ij} = h_1, h_2, h_3,$  or  $h_4$ , if the states  $i$  and  $j$  are related to each other by a  $120^\circ$  rotation around the 1, 2, 3, or 4 axis. These axes are fixed in the crystal and they are shown in Fig. 2.  $H_x, H_y,$  and  $H_z$  denote the  $180^\circ$  rotations around the X, Y, and Z axes. The off-diagonal or overlap matrix elements of the Hamiltonian are all negative in the relevant case of small overlap. The Hamiltonian matrix  $\mathcal{H}_{ij}$  (see Table II) in the part of Hilbert space which contains only the 12 pocket states  $|\varphi_i\rangle$  thus may be read off from Figs. 2 and 3.  $\mathcal{H}_{ij}$  may be block diagonalized by the unitary transformation  $|\xi_\mu\rangle = \sum_i a_{\mu i} |\varphi_i\rangle$ , with the matrix  $a$  from Table III. One obtains a singlet symmetrical ground state  $|\xi_{12}\rangle$ , with energy  $E_{12} = E_A = \langle \xi_{12} | \mathcal{H} | \xi_{12} \rangle = D + H + 2h$ , and a doublet state ( $|\xi_1\rangle$  and  $|\xi_2\rangle$ ), with energy  $E_1 = E_2 = E_B = D + H - h$ . Here we have used the notation  $H = H_x + H_y + H_z$ , and  $h = h_1 + h_2 + h_3 + h_4$ . Furthermore  $\mathcal{H}_{\mu\nu}$  contains three identical  $3 \times 3$  blocks  $\mathcal{H}$  of nonzero elements

$$\hat{\mathcal{H}} = \begin{pmatrix} D + H_x - H_y - H_z & -h_1 - h_2 + h_3 + h_4 & -h_1 + h_2 - h_3 + h_4 \\ -h_1 - h_2 + h_3 + h_4 & D - H_x + H_y - H_z & +h_1 - h_2 - h_3 + h_4 \\ -h_1 + h_2 - h_3 + h_4 & +h_1 - h_2 - h_3 + h_4 & D - H_x - H_y + H_z \end{pmatrix}. \quad (3.1)$$

TABLE II. Hamiltonian matrix  $\mathcal{H}_{ij}$  for the pocket states  $|\varphi_i\rangle$ .  $D$  is the diagonal matrix element.  $H_x, H_y,$  and  $H_z$  are the overlap matrix elements for  $180^\circ$  rotations around the  $X, Y,$  and  $Z$  axes, respectively. The matrix elements for  $120^\circ$  rotations around the 1, 2, 3, and 4 axes are denoted by  $h_1, h_2, h_3,$  and  $h_4$ . The rotation axes are fixed in the crystal reference system and are defined in Fig. 2.

$D$	$H_x$	$H_y$	$H_z$	$h_4$	$h_3$	$h_1$	$h_2$	$h_4$	$h_2$	$h_3$	$h_1$
$H_x$	$D$	$H_z$	$H_y$	$h_2$	$h_1$	$h_3$	$h_4$	$h_3$	$h_1$	$h_4$	$h_2$
$H_y$	$H_z$	$D$	$H_x$	$h_3$	$h_4$	$h_2$	$h_1$	$h_1$	$h_3$	$h_2$	$h_4$
$H_z$	$H_y$	$H_x$	$D$	$h_1$	$h_2$	$h_4$	$h_3$	$h_2$	$h_4$	$h_1$	$h_3$
$h_4$	$h_2$	$h_3$	$h_1$	$D$	$H_x$	$H_y$	$H_z$	$h_4$	$h_3$	$h_1$	$h_2$
$h_3$	$h_1$	$h_4$	$h_2$	$H_x$	$D$	$H_z$	$H_y$	$h_2$	$h_1$	$h_3$	$h_4$
$h_1$	$h_3$	$h_2$	$h_4$	$H_y$	$H_z$	$D$	$H_x$	$h_3$	$h_4$	$h_2$	$h_1$
$h_2$	$h_4$	$h_1$	$h_3$	$H_z$	$H_y$	$H_x$	$D$	$h_1$	$h_2$	$h_4$	$h_3$
$h_4$	$h_3$	$h_1$	$h_2$	$h_4$	$h_2$	$h_3$	$h_1$	$D$	$H_x$	$H_y$	$H_z$
$h_2$	$h_1$	$h_3$	$h_4$	$h_3$	$h_1$	$h_4$	$h_2$	$H_x$	$D$	$H_z$	$H_y$
$h_3$	$h_4$	$h_2$	$h_1$	$h_1$	$h_3$	$h_2$	$h_4$	$H_y$	$H_z$	$D$	$H_x$
$h_1$	$h_2$	$h_4$	$h_3$	$h_2$	$h_4$	$h_1$	$h_3$	$H_z$	$H_y$	$H_x$	$D$

One obtains the same  $3 \times 3$  matrix  $\hat{\mathcal{K}}$  for the following groups of states:  $(\xi_3, \xi_4, \xi_5), (\xi_6, \xi_7, \xi_8),$  and  $(\xi_9, \xi_{10}, \xi_{11})$ . All other elements of  $\mathcal{K}_{\mu\nu}$  are zero. The diagonalization of  $\mathcal{K}$  thus yields a singlet state with energy  $E_A$ , a doublet state with energy  $E_E$ , and three triplet states with energies  $E_{T1}, E_{T2},$  and  $E_{T3}$  as shown in Fig. 4.  $E_{T1}, E_{T2},$  and  $E_{T3}$  might be obtained from a diagonalization of  $\hat{\mathcal{K}}$ . Explicit expressions are, however, quite complicated and therefore do not yield much insight.

A general conclusion concerning the relative importance of  $H$  and  $h$  may, however, be drawn

without explicitly diagonalizing  $\hat{\mathcal{K}}$ . From the invariance of the trace of a matrix under unitary transformations and from Table II one obtains  $\sum E_i = 12D$ . Knowing  $E_A$  and  $E_E$  one concludes that the nine  $T$  states must be centered at  $C_T = D - \frac{1}{3}H$ . The average transition energy from the  $A$  state to the  $T$  states therefore is  $2/3H - 2h$ , and the average transition energy from the  $T$  states to the  $E$  state is  $2/3H - h$  (see Fig. 4). For the ratio of the transition energies one therefore finds

$$R = (2H - 6h)/(2H - 3h). \tag{3.2}$$

TABLE III. Matrix  $a_{\mu i}$  which transforms the Hamiltonian  $\mathcal{H}_{ij}$  into the block diagonal form  $\mathcal{K}_{\mu\nu}$ .  $a = 1/2\sqrt{3}, c = \frac{1}{2}, \bar{c} = -\frac{1}{2}, \epsilon = \frac{1}{2}(-1 + \sqrt{3}i), \bar{\epsilon} = \frac{1}{2}(-1 - \sqrt{3}i)$ .

$a$	$a$	$a$	$a$	$\epsilon$	$\epsilon$	$\epsilon$	$\epsilon$	$\bar{\epsilon}$	$\bar{\epsilon}$	$\bar{\epsilon}$	$\bar{\epsilon}$
$a$	$a$	$a$	$a$	$\bar{\epsilon}$	$\bar{\epsilon}$	$\bar{\epsilon}$	$\bar{\epsilon}$	$\epsilon$	$\epsilon$	$\epsilon$	$\epsilon$
$c$	$c$	$\bar{c}$	$\bar{c}$	0	0	0	0	0	0	0	0
0	0	0	0	0	0	0	0	$c$	$\bar{c}$	$c$	$\bar{c}$
0	0	0	0	$c$	$\bar{c}$	$\bar{c}$	$c$	0	0	0	0
0	0	0	0	$c$	$c$	$\bar{c}$	$\bar{c}$	0	0	0	0
$c$	$\bar{c}$	$c$	$\bar{c}$	0	0	0	0	0	0	0	0
0	0	0	0	0	0	0	0	$c$	$\bar{c}$	$\bar{c}$	$c$
0	0	0	0	0	0	0	0	$c$	$c$	$\bar{c}$	$\bar{c}$
0	0	0	0	$c$	$\bar{c}$	$c$	$\bar{c}$	0	0	0	0
$c$	$\bar{c}$	$\bar{c}$	$c$	0	0	0	0	0	0	0	0
$a$	$a$	$a$	$a$	$a$	$a$	$a$	$a$	$a$	$a$	$a$	$a$

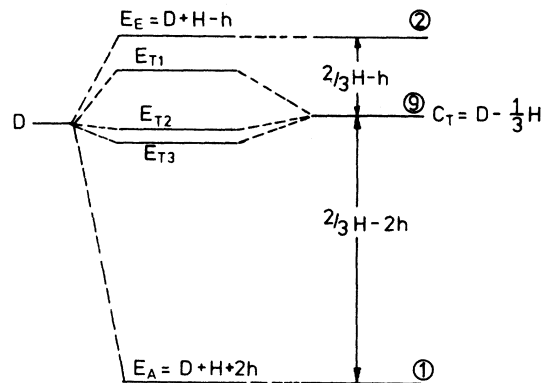


FIG. 4. Schematic drawing of the spectrum of the rotational Hamiltonian  $\mathcal{K}_{\mu\nu}$ .  $H = H_x + H_y + H_z, h = h_1 + h_2 + h_3 + h_4$ . The positions of  $E_{T1}, E_{T2},$  and  $E_{T3}$  may be obtained from the diagonalization of  $\mathcal{K}$  [Eq. (3.1)]. Their center of mass  $C_T$  is determined from the invariance of the trace.

The experimental value of  $R$  can be calculated from Table I and it is found to be equal to 2 with high precision for both  $\text{NH}_4^+\text{ClO}_4^-$  and  $(\text{NH}_4^+)_2\text{SnCl}_6^{--}$ . We thus conclude that  $|H| \ll |h|$  and with the knowledge that the overlap matrix elements are all negative one finds:

$$|H_x|, |H_y|, |H_z| \ll |h_1 + h_2 + h_3 + h_4|. \quad (3.3)$$

Inequality (3.3) is not very surprising. The pocket state wave functions are falling off rapidly outside the potential pockets and the overlap matrix elements should be strongly decreasing with increasing distance between the pockets. The corresponding states for  $H$  are  $180^\circ$  apart, whereas the states for one of the  $h$  elements are only  $120^\circ$  apart.

For all practical purposes one may therefore simplify  $\mathcal{H}$  by putting  $H_x$ ,  $H_y$ , and  $H_z$  equal to zero. For a tetrahedral crystal field, e.g., in  $(\text{NH}_4^+)_2\text{SnCl}_6^{--}$  or in phase II of solid  $\text{CH}_4$ , all four elements  $h_i$  are equal and therefore the three triplets coalesce into one ninefold degenerate level at an energy  $E_T = D$ .

In  $\text{NH}_4\text{ClO}_4$  where a mirror plane is the only symmetry element of the  $\text{NH}_4^+$  site, two of the four  $120^\circ$  overlap matrix elements are equal. If the orientation of the molecule is such, that the two threefold rotation axes 1 and 2 coincide with the mirror plane, then  $h_3 = h_4$ . Consequently  $\hat{\mathcal{H}}$  is simplified to

$$\hat{\mathcal{H}} = \begin{pmatrix} D & \gamma & -\alpha \\ \gamma & D & \alpha \\ -\alpha & \alpha & D \end{pmatrix}. \quad (3.4)$$

Here  $\alpha = h_1 - h_2$ , and  $\gamma = -h_1 - h_2 + 2h_3$ .  $\hat{\mathcal{H}}$  has the eigenvalues

$$\begin{aligned} E_{T_1} &= D - \frac{1}{2}\gamma + \left(\frac{1}{4}\gamma^2 + 2\alpha^2\right)^{1/2}, \\ E_{T_2} &= D - \frac{1}{2}\gamma - \left(\frac{1}{4}\gamma^2 + 2\alpha^2\right)^{1/2}, \\ E_{T_3} &= D + \gamma. \end{aligned} \quad (3.5)$$

These three eigenvalues in general are nondegenerate and we conclude that the additional degeneracy  $E_{T_2} = E_{T_3}$  in  $\text{NH}_4^+\text{ClO}_4^-$  is an *accidental* one.

Fitting the observed<sup>18</sup> transition frequencies in  $\text{NH}_4^+\text{ClO}_4^-$  to Eq. (3.5) one obtains the three remaining overlap matrix elements:  $h_1 = -0.038 \mu\text{eV}$ , and  $h_2 = h_3 = h_4 = -1.410 \mu\text{eV}$ . The equality of  $h_2$  with  $h_3$  and  $h_4$  is a consequence of the accidental degeneracy found in the experiment. The smallness of  $h_1$  at first hand is an astonishing fact. It shows that the barrier to rotation is quite high for one of the four threefold rotation axes, and low for the other three. This observation is at variance with the idea of one soft and three hard threefold rotation axes which has been used for

$\text{NH}_4^+\text{ClO}_4^-$  to explain NMR data.<sup>7</sup> The latter model predicts a fourfold ground state and an eightfold excited state with just one transition frequency.

The observation of three big and one small overlap matrix elements is however in excellent agreement with the structure determination of Choi, Prask, and Prince.<sup>26</sup> These authors have determined the principal axes of rotation of the  $\text{NH}_4$  tetrahedron together with the librational amplitudes around these axes:  $\Phi_i = 20.8^\circ$ ,  $11.4^\circ$ , and  $10.1^\circ$ . In a harmonic model the amplitudes  $\Phi_i$  are proportional to the inverse fourth root of the force constants  $K_i$

$$\Phi_i \sim K_i^{-0.25}. \quad (3.6)$$

The force constants for rotations around the principal axes thus relate to each other as 1:11:18. Projecting on the rotation axes 1, 2, 3, and 4 of Fig. 2 one obtains the following ratio of harmonic force constants around the threefold symmetry axes:

$$K_1 : K_2 : K_3 : K_4 = 16.2 : 7.4 : 8.0 : 8.0. \quad (3.7)$$

Equation (3.7) shows that axis 1 is a hard rotation axis, whereas the other three axes are soft with almost equal rotational force constants. Consequently the matrix element  $h_1$  is expected to be much smaller than  $h_2$ ,  $h_3$ , and  $h_4$ . The tunneling experiment and the structure determination thus are in perfect agreement with each other.

#### B. Proton spin states and symmetry

So far we have restricted ourselves to the rotational wave function of a molecule; the nuclear spin states have not yet been included into the considerations. There are 16 spin states  $|\mu_1\mu_2\mu_3\mu_4\rangle$  for a system of four protons.  $\mu_1$ ,  $\mu_2$ ,  $\mu_3$ , and  $\mu_4$  denote the  $z$  component of the nuclear spin of *particle* number 1, 2, 3, and 4, respectively.  $\langle I_x \rangle = +\frac{1}{2}$  is denoted by  $\alpha$ , and  $\langle I_x \rangle = -\frac{1}{2}$  by  $\beta$ . All 16 states are shown in Table IV. The Hamiltonian  $\mathcal{H} = T + V$  does not involve the spin coordinates, and consequently there is also no coupling of the spins with the rotational degrees of freedom. The total wave functions  $|\psi_m\rangle$  therefore may be constructed from products of rotational wave functions (pocket states) and spin-wave functions

$$|\psi_\alpha\rangle = \sum_{i, \mu_1\mu_2\mu_3\mu_4} A_{i, \mu_1\mu_2\mu_3\mu_4}^\alpha |\varphi_i\rangle |\mu_1\mu_2\mu_3\mu_4\rangle. \quad (3.8)$$

All possible 192 products  $|\varphi_i\rangle |\mu_1\mu_2\mu_3\mu_4\rangle$  are contained in Table IV. According to the discussion at the beginning of this chapter only those wave functions  $|\psi_\alpha\rangle$  which are totally symmetric under the 12 symmetry operation of the group, are physically allowed wave functions. The symmetry operations  $R_i$  are the 12 even permutations of the four protons. If such a permutation is applied to one the

TABLE IV. In this table there is one place for each of the 192 products of the type  $|\varphi_i\rangle|\mu_1\mu_2\mu_3\mu_4\rangle$ . The symmetry operations only rearrange the products within 16 groups. The number at each position shows to which group the product belongs.

$I_z^t$	Spin states $ \mu_1\mu_2\mu_3\mu_4\rangle$	Pocket states $ \varphi_i\rangle$											
		1	2	3	4	5	6	7	8	9	10	11	12
+2	$ \alpha\alpha\alpha\alpha\rangle$	1	1	1	1	1	1	1	1	1	1	1	1
+1	$ \beta\alpha\alpha\alpha\rangle$	2	5	4	3	4	3	2	5	3	4	5	2
	$ \alpha\beta\alpha\alpha\rangle$	3	4	5	2	2	5	4	3	4	3	2	5
	$ \alpha\alpha\beta\alpha\rangle$	4	3	2	5	3	4	5	2	2	5	4	3
	$ \alpha\alpha\alpha\beta\rangle$	5	2	3	4	5	2	3	4	5	2	3	4
0	$ \alpha\alpha\beta\beta\rangle$	6	7	7	6	10	11	10	11	9	9	8	8
	$ \beta\beta\alpha\alpha\rangle$	7	6	6	7	11	10	11	10	8	8	9	9
	$ \alpha\beta\beta\alpha\rangle$	8	8	9	9	7	6	6	7	11	10	11	10
	$ \beta\alpha\alpha\beta\rangle$	9	9	8	8	6	7	7	6	10	11	10	11
	$ \alpha\beta\alpha\beta\rangle$	10	11	10	11	9	9	8	8	6	7	7	6
	$ \beta\alpha\beta\alpha\rangle$	11	10	11	10	8	8	9	9	7	6	6	7
-1	$ \alpha\beta\beta\beta\rangle$	12	15	14	13	14	13	12	15	13	14	15	12
	$ \beta\alpha\beta\beta\rangle$	13	14	15	12	12	15	14	13	14	13	12	15
	$ \beta\beta\alpha\beta\rangle$	14	13	12	15	13	14	15	12	12	15	14	13
	$ \beta\beta\beta\alpha\rangle$	15	12	13	14	15	12	13	14	15	12	13	14
-2	$ \beta\beta\beta\beta\rangle$	16	16	16	16	16	16	16	16	16	16	16	

products  $|\varphi_i\rangle|\mu_1\mu_2\mu_3\mu_4\rangle$ , this product is transformed into another one. The application of all the symmetry operations on all products  $|\varphi_i\rangle|\mu_1\mu_2\mu_3\mu_4\rangle$  allows a separation of these products into 16 groups of 12 products each. If one applies any symmetry operation (including of course the identity operation) to all elements within a group, one recreates each product within the group exactly once. The membership in one of the 16 groups is denoted by a number  $m=1, 2, \dots, 16$  in Table IV. A sum over all 12 members of a group  $m$  is invariant under each of the symmetry operations. We therefore get 16 totally symmetric wave functions by summing over the 12 members of each group:

$$|\chi_m\rangle = \frac{1}{\sqrt{12}} \sum_{\text{group } m} |\varphi_i\rangle|\mu_1\mu_2\mu_3\mu_4\rangle. \quad (3.9)$$

As an example  $\chi_2$  is written down explicitly:

$$|\chi_2\rangle = (1/\sqrt{12}) [ +|\beta\alpha\alpha\alpha\rangle(|\varphi_1\rangle + |\varphi_7\rangle + |\varphi_{12}\rangle) + |\alpha\beta\alpha\alpha\rangle(|\varphi_4\rangle + |\varphi_5\rangle + |\varphi_{11}\rangle) + |\alpha\alpha\beta\alpha\rangle(|\varphi_3\rangle + |\varphi_8\rangle + |\varphi_9\rangle) + |\alpha\alpha\alpha\beta\rangle(|\varphi_2\rangle + |\varphi_6\rangle + |\varphi_{10}\rangle) ]. \quad (3.10)$$

The states  $|\chi_m\rangle$  are no eigenstates of the problem. It has already been remarked however, that the Hamiltonian does not involve the spin coordinates. It therefore does not connect states with different  $z$  components of the total spin  $I_z^t = I_z^1 + I_z^2 + I_z^3 + I_z^4$ . Consequently the Hamiltonian matrix is already block diagonal with an eigenvalue  $E_A = D + H + 2h$  for both the states  $|\chi_1\rangle$  and  $|\chi_{16}\rangle$ , with  $I_z^t = \pm 2$ . For  $I_z^t = +1$  ( $|\chi_2\rangle, |\chi_3\rangle, |\chi_4\rangle, |\chi_5\rangle$ ), and for  $I_z^t = -1$  ( $|\chi_{12}\rangle, |\chi_{13}\rangle, |\chi_{14}\rangle, |\chi_{15}\rangle$ ), there are two identical blocks  $\mathcal{K}_4$  in  $\mathcal{K}_{mn}$ :

$$\mathcal{K}_4 = \begin{bmatrix} D + 2h_1 & H_x + h_3 + h_4 & H_y + h_4 + h_2 & H_x + h_2 + h_3 \\ H_x + h_3 + h_4 & D + 2h_2 & H_x + h_1 + h_4 & H_y + h_1 + h_3 \\ H_y + h_4 + h_2 & H_x + h_1 + h_4 & D + 2h_3 & H_x + h_1 + h_2 \\ H_x + h_2 + h_3 & H_y + h_1 + h_3 & H_x + h_1 + h_2 & D + 2h_4 \end{bmatrix}. \quad (3.11)$$

Each of the two blocks  $\mathcal{K}_4$  contains the energy eigenvalues  $E_A, E_{T_1}, E_{T_2}$ , and  $E_{T_3}$  which we have already encountered in Sec. III A. For the six wave functions  $|\chi_6\rangle, |\chi_7\rangle, |\chi_8\rangle, |\chi_9\rangle, |\chi_{10}\rangle$ , and  $|\chi_{11}\rangle$ , with  $I_z^t = 0$ , one obtains the block  $\mathcal{K}_6$ :

$$\mathcal{K}_8 = \begin{bmatrix} D+H_x & H_x+H_y & h_1+h_3 & h_2+h_4 & h_1+h_4 & h_2+h_3 \\ H_x+H_y & D+H_x & h_2+h_4 & h_1+h_3 & h_2+h_3 & h_1+h_4 \\ h_1+h_3 & h_2+h_4 & D+H_x & H_y+H_x & h_1+h_2 & h_3+h_4 \\ h_2+h_4 & h_1+h_2 & H_y+H_x & D+H_x & h_3+h_4 & h_1+h_2 \\ h_1+h_4 & h_2+h_3 & h_1+h_2 & h_3+h_4 & D+H_y & H_x+H_x \\ h_2+h_3 & h_1+h_4 & h_3+h_4 & h_1+h_2 & H_x+H_x & D+H_y \end{bmatrix}. \quad (3.12)$$

$\mathcal{K}_8$  contains the eigenvalues  $E_A$ ,  $E_{T_1}$ ,  $E_{T_2}$ ,  $E_{T_3}$ , and in addition to that a doubly degenerate level with energy  $E_E = D + H - h$ .

The only advantage gained with the correctly symmetrized functions  $|\chi_m\rangle$ , in comparison with the pure rotational functions  $|\varphi_i\rangle$ , seems to be the correct result that the  $A$  state is fivefold degenerate. For the calculation of neutron scattering matrix elements in Sec. IV the correctly symmetrized wave functions will however be indispensable.

It should be remarked that the 16 functions  $|\chi_1\rangle$ ,  $|\chi_2\rangle, \dots, |\chi_{16}\rangle$  have a simple interpretation in terms of wave functions  $[\mu_1\mu_2\mu_3\mu_4]$ . Here  $\mu_1$  denotes the spin state of the proton at *site* (or *position*) No. 1 irrespective if it is particle number 1, 2, 3, or 4 which sits at this position. Similarly  $\mu_2$ ,  $\mu_3$ , and  $\mu_4$  denote the spin states of the particles at positions 2, 3, and 4, respectively. An angular bracket [ has been used to distinguish these states which define the proton spin state at a *site*, from the

states  $|\mu_1\mu_2\mu_3\mu_4\rangle$  which define the spin states of identified *particles*. By definition the functions  $[\mu_1\mu_2\mu_3\mu_4]$  are totally symmetric under the particle exchange operator. It does not matter that  $[\mu_1\mu_2\mu_3\mu_4]$  is also symmetric under the exchange of just two particles (odd permutations) because we have excluded these operations from the start. Equation (3.10) now becomes simply

$$|\chi_2\rangle = [\beta\alpha\alpha\alpha]. \quad (3.10')$$

The step from (3.10) to (3.10') is easily verified from the definition of the states  $|\mu_1\mu_2\mu_3\mu_4\rangle$  given at the beginning of Sec. III B) and from Fig. 3. All 16 functions  $[\mu_1\mu_2\mu_3\mu_4]$  are shown in Fig. 5.

The question why we have not started the whole paper with the apparently very simple wave functions  $[\mu_1\mu_2\mu_3\mu_4]$  is now self-imposing. The question can be put aside with the remark that a lot of intuition would be required to determine the Hamiltonian matrix ( $\mathcal{K}_4, \mathcal{K}_6$ ) directly from the func-

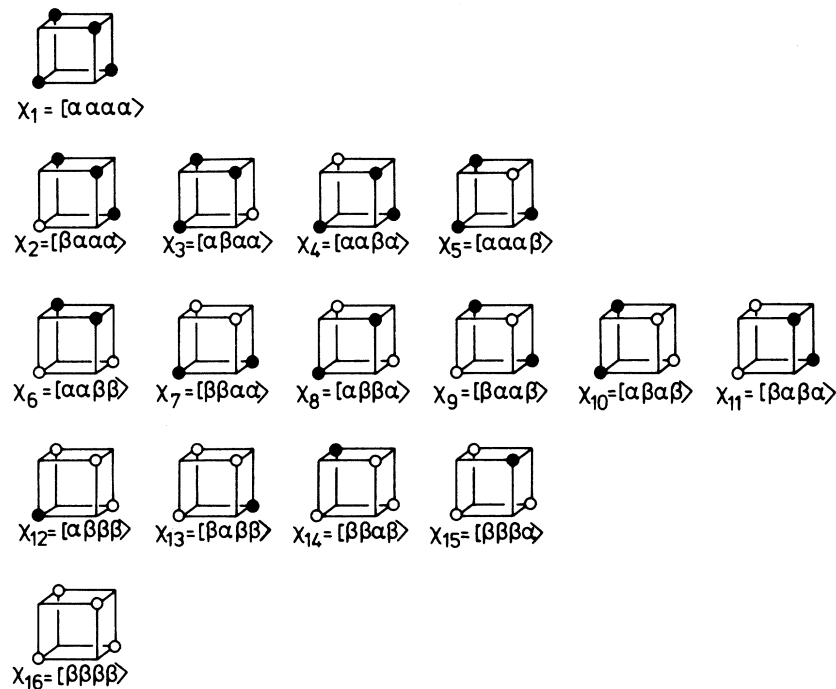


FIG. 5. Sixteen totally symmetric wave functions  $[\mu_1\mu_2\mu_3\mu_4]$  which define the spin states at the four-particle positions in the crystal reference system. The particles in the positions are not identified. Open circles denote spin down, full circles spin up.



TABLE V. Unitary matrix  $b_{\alpha m}$  of Eq. (3.13) which transforms from the states  $|\chi_m\rangle = [\mu_1\mu_2\mu_3\mu_4]$  to the eigenstates of the ammonium perchlorate system.  $I^t$  and  $I_z^t$  are the total nuclear spin and its  $z$  component.  $t=1/\sqrt{12}$ ,  $h=\frac{1}{2}$ ,  $s=1/\sqrt{6}$ .

$I^t$	$I_z^t$	$\alpha$	$m$																
			1	2	3	4	5	6	7	8	9	10	11	12	13	14	15	16	
0	0	1	0	0	0	0	0	0	+2t	+2t	-t	-t	-t	-t	0	0	0	0	0
	0	2	0	0	0	0	0	0	0	0	+h	+h	-h	-h	0	0	0	0	0
1	+1	3	0	+3t	-t	-t	-t	0	0	0	0	0	0	0	0	0	0	0	0
	0	4	0	0	0	0	0	0	+s	-s	+s	-s	+s	-s	0	0	0	0	0
	-1	5	0	0	0	0	0	0	0	0	0	0	0	0	+3t	-t	-t	-t	0
1	+1	6	0	0	+2s	-s	-s	0	0	0	0	0	0	0	0	0	0	0	0
	0	7	0	0	0	0	0	+2t	-2t	-t	+t	-t	+t	0	0	0	0	0	0
	-1	8	0	0	0	0	0	0	0	0	0	0	0	0	+2s	-s	-s	0	0
	+1	9	0	0	0	+z	-z	0	0	0	0	0	0	0	0	0	0	0	0
	0	10	0	0	0	0	0	0	0	0	+h	-h	-h	+h	0	0	0	0	0
	-1	11	0	0	0	0	0	0	0	0	0	0	0	0	0	0	+z	-z	0
2	+2	12	1	0	0	0	0	0	0	0	0	0	0	0	0	0	0	0	0
	+1	13	0	+h	+h	+h	+h	0	0	0	0	0	0	0	0	0	0	0	0
	0	14	0	0	0	0	0	+s	+s	+s	+s	+s	+s	0	0	0	0	0	0
	-1	15	0	0	0	0	0	0	0	0	0	0	0	+h	+h	+h	+h	0	0
	-2	16	0	0	0	0	0	0	0	0	0	0	0	0	0	0	0	0	1

tions  $[\mu_1\mu_2\mu_3\mu_4]$ . We have derived it from the relation of the pocket states  $|\varphi_i\rangle$  to each other.

From a diagonalization of  $\mathcal{H}_4$  and  $\mathcal{H}_8$  one obtains the eigenfunctions  $|\psi_\alpha\rangle$ . This diagonalization is performed explicitly for a special case that comes close to the real situation in  $\text{NH}_4^+\text{ClO}_4^-$ . We put  $h_2=h_3=h_4$ , and  $h_1=0$ . (In ammonium perchlorate  $h_1$  is smaller than the other  $h_i$  by roughly a factor 30–40.) One finds the wave functions

$$|\psi_\alpha\rangle = \sum_{m=1}^{16} b_{\alpha m} |\chi_m\rangle, \quad (3.13)$$

where the unitary matrix  $b_{\alpha m}$  is given in Table V. The states with  $\alpha=1, 2$  belong to the doubly degenerate  $E$  level with energy  $E_E = D - 3h_2$ . There is one triplet ( $\alpha=3-5$ ) at the energy  $E_{T_1} = D - 2h_2$ . For  $h_2=h_3=h_4$  the two triplets ( $\alpha=6-8$ ) and ( $\alpha=9-11$ ) have the same energy  $E_{T_2} = E_{T_3} = D + h_2$ . Five states ( $\alpha=12-16$ ) have the energy  $E_A = D + 6h_2$ .

#### IV. EVALUATION OF THE NEUTRON SCATTERING CROSS SECTION

From the discussion of Sec. II it is clear that each state  $|\Psi_\alpha\rangle$  of the system is a product of single-molecule states  $|\psi_{n\alpha}\rangle$ . In the initial mixture of states, characterized by the probabilities  $P_\alpha$ , there

are no correlations between the single-molecule states  $|\psi_{n_1\alpha_1}\rangle$  and  $|\psi_{n_2\alpha_2}\rangle$  for different molecules  $n_1$  and  $n_2$ . Consequently the spin states of two protons at the sites  $R_{n_1\gamma_1}$  and  $R_{n_2\gamma_2}$  are not correlated if  $n_1 \neq n_2$ . In the neutron scattering cross section of Eq. (1.1)

$$\begin{aligned} \frac{d^2\sigma}{d\Omega d\omega} &= \sum_{\mu\mu'} \sum_{\alpha\alpha'} P_\mu P_\alpha \delta(\omega - \omega_{\alpha,\alpha'}) \\ &\times \sum_{n_1 n_2 \gamma_1 \gamma_2} \langle \mu \Psi_\alpha | A^{n_1 \gamma_1} e^{-i\vec{Q} \cdot \vec{R}_{n_1 \gamma_1}} | \mu' \Psi_{\alpha'} \rangle \\ &\times \langle \mu' \Psi_{\alpha'} | A^{n_2 \gamma_2} e^{i\vec{Q} \cdot \vec{R}_{n_2 \gamma_2}} | \mu \Psi_\alpha \rangle. \end{aligned} \quad (4.1)$$

with  $\vec{Q} = \vec{k} - \vec{k}'$ , the sum over  $n_1 n_2 \gamma_1 \gamma_2$  is used in its interpretation as a double sum over the lattice sites  $n\gamma$  which are occupied by protons. With no correlations between the spin states of protons at different molecules, the matrix elements of  $A^{n_1 \gamma_1}$  and  $A^{n_2 \gamma_2}$  may be replaced by averages, if  $n_1 \neq n_2$ . The scattering cross section separates into two parts:

$$\frac{d^2\sigma}{d\Omega d\omega} = \frac{d^2\sigma_d}{d\Omega d\omega} + \frac{d^2\sigma_s}{d\Omega d\omega}, \quad (4.2)$$

with

$$\frac{d^2\sigma_d}{d\Omega d\omega} = \sum_{\mu\mu'} \sum_{\alpha\alpha'} P_\mu P_{\alpha'} \delta(\omega - \omega_{\alpha,\alpha'}) \bar{A}^2 \sum_{n_1 n_2 \gamma_1 \gamma_2} \langle \mu \Psi_\alpha | e^{-i\vec{Q}\cdot\vec{R}_{n_1\gamma_1}} | \mu' \Psi_{\alpha'} \rangle \langle \mu' \Psi_{\alpha'} | e^{i\vec{Q}\cdot\vec{R}_{n_2\gamma_2}} | \mu \Psi_\alpha \rangle \quad (4.3)$$

and

$$\frac{d^2\sigma_s}{d\Omega d\omega} = \sum_{\mu\mu'} \sum_{\alpha\alpha'} P_\mu P_{\alpha'} \delta(\omega - \omega_{\alpha,\alpha'}) \sum_{n\gamma_1\gamma_2} \langle \mu \Psi_\alpha | (A^{n\gamma_1} - \bar{A}) e^{-i\vec{Q}\cdot\vec{R}_{n\gamma_1}} | \mu' \Psi_{\alpha'} \rangle \langle \mu' \Psi_{\alpha'} | (A^{n\gamma_2} - \bar{A}) e^{i\vec{Q}\cdot\vec{R}_{n\gamma_2}} | \mu \Psi_\alpha \rangle. \quad (4.4)$$

The mean scattering length  $\bar{A}$  is defined by an average over the spin states  $|\nu\rangle$  at the  $4N$  proton sites:

$$\bar{A} = \sum_{\mu\mu'} \sum_{\nu\nu'=\pm 1/2} P_\mu P_{\nu'} \frac{1}{4N} \sum_{n\gamma} \langle \nu' \mu' | A^{n\gamma} | \nu \mu \rangle, \quad (4.5)$$

where  $P_\nu$  is the probability to find the proton at position  $n\gamma$  in the state  $|\nu\rangle$ . For the unpolarized sample under consideration one finds

$$\bar{A} = a_{\text{coh}}. \quad (4.6)$$

The scattering due to  $\sigma_d$  is coherent. The elastic intensity goes into the Bragg peaks, the inelastic intensity is restricted by the conservation laws of energy and quasimomentum. We shall concentrate on  $\sigma_s$  which is a sum over the individual scattering intensities from the  $N$  molecules.  $\sigma_s$  no longer contains the spin-independent scattering length  $a_{\text{coh}}$ . Nevertheless the scattering is coherent with respect to the protons of a single molecule.

In (4.4) we replace  $|\Psi_\alpha\rangle$  by a product of single-molecule states  $|\psi_{n\alpha}\rangle$ , the energy difference  $\hbar\omega_{\alpha,\alpha'}$  by  $\hbar\omega_{\alpha,\alpha'}$ , and the probability  $P_\alpha$  by  $p_\alpha$ , the probability to find a molecule in the state  $|\psi_\alpha\rangle$ :

$$\frac{d^2\sigma_s}{d\Omega d\omega} = \sum_n \sum_{\mu\mu'} \sum_{\alpha\alpha'} P_\mu p_\alpha \delta(\omega - \omega_{\alpha,\alpha'}) |A_{\mu'\alpha',\mu\alpha}^n|^2, \quad (4.7)$$

where

$$A_{\mu'\alpha',\mu\alpha}^n = \sum_{\gamma=1}^4 \langle \mu' \psi_{n\alpha'} | (A^{n\gamma} - \bar{A}) e^{i\vec{Q}\cdot\vec{R}_{n\gamma}} | \mu \psi_\alpha \rangle \quad (4.8)$$

for the calculation of the scattering matrix element  $A_{\mu'\alpha',\mu\alpha}^n$  the pocket states  $|\mu_1\mu_2\mu_3\mu_4\rangle$ , or equivalently  $|\chi_m\rangle = |\mu_1\mu_2\mu_3\mu_4\rangle$ , are approximated by  $\delta$  functions in the equilibrium orientation. It is then easy to calculate the matrix elements:

$$B_{m'\mu',m\mu}^n = \sum_{\gamma=1}^4 \langle \mu' | \langle \chi_{m'} | (A^{n\gamma} - \bar{A}) e^{i\vec{Q}\cdot\vec{R}_{n\gamma}} | \chi_m \rangle | \mu \rangle. \quad (4.9)$$

In

$$A^{n\gamma} - \bar{A} = 2a_{\text{inc}}/[I(I+1)]^{1/2} \vec{S} \cdot \vec{I}_{n\gamma}$$

we substitute

$$\vec{S} \cdot \vec{I}_{n\gamma} = S_z I_{n\gamma z} + \frac{1}{2} (S_+ I_{n\gamma-} + S_- I_{n\gamma+}). \quad (4.10)$$

$B_{m'\mu',m\mu}^n$  is a sum of exponential terms  $G_\gamma$ :

$$G_\gamma = e^{i\vec{Q}\cdot\vec{R}_{n\gamma}^0}, \quad (4.11)$$

where  $R_{n\gamma}^0$  is one of the four equilibrium sites occupied by the protons of the  $n$ th molecule. The effect of the  $\delta$ -function approximation for the wave function is the replacement of the expectation value  $\langle e^{i\vec{Q}\cdot\vec{R}_{n\gamma}} \rangle$  in the state  $|\chi_m\rangle$  by  $e^{i\vec{Q}\cdot\vec{R}_{n\gamma}^0}$ , the value at the equilibrium position. The approximation is valid if  $(\vec{Q}\cdot\vec{R}_{n\gamma})^2 < 1$ . In  $\text{NH}_4^+\text{ClO}_4^-$  with a librational amplitude of  $20^\circ$  this is the case for  $Q < 1.5 \text{ \AA}^{-1}$ . For larger momentum transfers the form factor of the cap-shaped density distribution becomes appreciable and a  $\delta$  function no longer is a good approximation. The theory should then be extended to include the librational amplitude of the pocket state wave functions.

The matrix elements  $B_{m'\mu',m\mu}^n$  for transitions where the neutron spin has been flipped from up to down ( $\mu = \alpha, \mu' = \beta$ ) are listed in the lower left-hand corner of Table VI. The ones where the neutron spin has been flipped from down to up ( $\mu = \beta, \mu' = \alpha$ ) are found in the upper right-hand corner of the same table. The non-spin-flip scattering involves only diagonal matrix elements which have been listed in Table VII.

$A_{\mu'\alpha',\mu\alpha}^n$  is then obtained from the transformation (3.13)

$$A_{\mu'\alpha',\mu\alpha}^n = \sum_{mm'} b_{m'\alpha'}^* b_{m\alpha} B_{m'\mu',m\mu}^n. \quad (4.12)$$

Equation (4.7) can now be evaluated. In the limit of  $kT$  large compared with  $\Delta\omega$  (the splitting in the ground-state multiplet) the probabilities for the initial states are all equal:  $p_\alpha = \frac{1}{16}$ . [In  $(\text{NH}_4)_2\text{SnCl}_6$  and  $\text{NH}_4^+\text{ClO}_4^-$  this is very well fulfilled with  $\Delta\omega/k \approx 0.1 \text{ K}$ , and  $4 < T < 80 \text{ K}$ .] For an unpolarized neutron beam  $P_\mu$  is equal to  $\frac{1}{2}$  for both values of  $\mu$ . To calculate the intensities in the different lines, the sums in Eq. (4.7) are performed over the initial states  $|\psi_\alpha\rangle$  and final states  $|\psi_{\alpha'}\rangle$  which belong to the concerned energy levels. The resulting angle-dependent cross sections are given in Table VIII. In agreement with the experimental results the scattering from the  $A$  level into the  $E$  level is not allowed. The intensities for the reverse processes are the same. The last five entries in Table VIII refer to the elastic line.

With the definition of  $G_\gamma$  [see Eq. (4.11)] the dependence of these cross sections on  $\theta_Q$  and  $\varphi_Q$ , the polar angles of the scattering vector  $\vec{Q}$ , is easily calculated. The angular dependence of

TABLE VI. Spin-flip scattering matrix elements

$$B_{m'\mu', m\mu} = \sum_{\gamma} \langle \mu' | \chi_{m'} | (A^{\mu\gamma} - \bar{A}) e^{i\vec{Q} \cdot \vec{R}_{m\gamma}} | \chi_m | \mu \rangle$$

are obtained from this table by a multiplication of  $G_{\gamma} = e^{(i\vec{Q} \cdot \vec{R}_{m\gamma}^0)}$ , with  $2a_{\text{inc}}/\sqrt{3}$ . Elements where the neutron spin is flipped down ( $\mu' = \beta, \mu = \alpha$ ) are found to the left and below of the main diagonal, elements where the neutron spin is flipped up ( $\mu' = \alpha, \mu = \beta$ ) are found to the right and above the main diagonal. The non-spin-flip matrix elements  $b_m = B_{m\mu, m\mu}$  with  $\mu = \alpha$  and  $\mu = \beta$  are found in Table VII.

$\chi'_1$	$\chi'_2$	$\chi'_3$	$\chi'_4$	$\chi'_5$	$\chi'_6$	$\chi'_7$	$\chi'_8$	$\chi'_9$	$\chi'_{10}$	$\chi'_{11}$	$\chi'_{12}$	$\chi'_{13}$	$\chi'_{14}$	$\chi'_{15}$	$\chi'_{16}$	
$b_1$	$G_1$	$G_2$	$G_3$	$G_4$	0	0	0	0	0	0	0	0	0	0	$\chi_1$	
$G_1$	$b_2$	0	0	0	0	$G_2$	0	$G_4$	0	$G_3$	0	0	0	0	$\chi_2$	
$G_2$	0	$b_3$	0	0	0	$G_1$	$G_3$	0	$G_4$	0	0	0	0	0	$\chi_3$	
$G_3$	0	0	$b_4$	0	$G_4$	0	$G_2$	0	0	$G_1$	0	0	0	0	$\chi_4$	
$G_4$	0	0	0	$b_5$	$G_3$	0	0	$G_1$	$G_2$	0	0	0	0	0	$\chi_5$	
0	0	0	$G_4$	$G_3$	$b_6$	0	0	0	0	0	$G_2$	$G_1$	0	0	$\chi_6$	
0	$G_2$	$G_1$	0	0	0	$b_7$	0	0	0	0	0	0	$G_4$	$G_3$	0	$\chi_7$
0	0	$G_3$	$G_2$	0	0	0	$b_8$	0	0	0	$G_4$	0	0	$G_1$	0	$\chi_8$
0	$G_4$	0	0	$G_1$	0	0	0	$b_9$	0	0	0	$G_3$	$G_2$	0	0	$\chi_9$
0	0	$G_4$	0	$G_2$	0	0	0	0	$b_{10}$	0	$G_3$	0	$G_1$	0	0	$\chi_{10}$
0	$G_3$	0	$G_1$	0	0	0	0	0	0	$b_{11}$	0	$G_4$	0	$G_2$	0	$\chi_{11}$
0	0	0	0	0	$G_2$	0	$G_4$	0	$G_3$	0	$b_{12}$	0	0	0	$G_1$	$\chi_{12}$
0	0	0	0	0	$G_1$	0	0	$G_3$	0	$G_4$	0	$b_{13}$	0	0	$G_2$	$\chi_{13}$
0	0	0	0	0	0	$G_4$	0	$G_2$	$G_1$	0	0	0	$b_{14}$	0	$G_3$	$\chi_{14}$
0	0	0	0	0	0	$G_3$	$G_1$	0	0	$G_2$	0	0	0	$b_{15}$	$G_4$	$\chi_{15}$
0	0	0	0	0	0	0	0	0	0	0	$G_1$	$G_2$	$G_3$	$G_4$	$b_{16}$	$\chi_{16}$

$d^2\sigma_g/d\Omega d\omega$  is pronounced, showing the importance of the interference terms for the scattering from the four protons within one molecule. The usual spin incoherence of the neutron scattering from protonic samples is due to the lack of knowledge concerning the proton spin states. For a tunneling line one has the information about the spins in the initial as well as in the final state. Therefore the protons within one molecule scatter coherently.

The effect of spin correlations on the neutron scattering cross section of gas phase methane has been studied a few years ago.<sup>27-30</sup> The influence of the spin correlations is only appreciable when the temperature is not very much larger than the level spacing of the free rotor spectrum. The theoretical studies have therefore been applied to the somewhat artificial situation of a methane gas at 10 K. The situation is quite different for strongly hindered molecules. The  $\vec{Q}$  dependence of their tunneling lines which is a spin-correlation effect, can be observed for temperatures that are much larger than the tunnel splitting. In  $(\text{NH}_4^+)_2\text{SnCl}_6^{--}$ , e.g., the splitting is of the order of 0.03 K. The  $Q$  de-

pendence of the scattering intensity exists in the whole temperature where the splitting has been observed, i.e., up to 80 K.

The angular dependence of the scattering cross section should be tested in a single-crystal neutron scattering experiment. When there is more than one  $\text{NH}_4^+$  group or  $\text{CH}_4$  molecule in the unit cell, as in  $\text{NH}_4^+\text{ClO}_4^-$ , the contributions from the differently oriented molecules have to be superposed. From such an experiment one may obtain information about the orientation of the tunneling group in the crystal. Deviations of the experimental results from the predictions of Table VIII, which will occur at high momentum transfers, contain information about the librational amplitudes in the pocket state wave functions.

A sum over all lines (elastic and inelastic) yields the total cross section  $\sigma_{\text{tot}} = 4Na_{\text{inc}}$  which does not depend on  $\vec{Q}$ , as the information about the spins in the initial and final state is not retained (incoherent scattering).

To compare the results of Table VIII with existing experiments on polycrystalline samples the

TABLE VII. Non-spin-flip scattering matrix elements  $B_{m\mu, m\mu}$  for  $\mu=\alpha$  and  $\mu=\beta$  differ in sign:  $B_{m\alpha, m\alpha} = b_m a_{1nc} / \sqrt{3}$ , and  $B_{m\beta, m\beta} = -b_m a_{1nc} / \sqrt{3}$ .

$m$	$b_m$
1	$+G_1 + G_2 + G_3 + G_4$
2	$-G_1 + G_2 + G_3 + G_4$
3	$+G_1 - G_2 + G_3 + G_4$
4	$+G_1 + G_2 - G_3 + G_4$
5	$+G_1 + G_2 + G_3 - G_4$
6	$+G_1 + G_2 - G_3 - G_4$
7	$-G_1 - G_2 + G_3 + G_4$
8	$+G_1 - G_2 - G_3 + G_4$
9	$-G_1 + G_2 + G_3 - G_4$
10	$+G_1 - G_2 + G_3 - G_4$
11	$-G_1 + G_2 - G_3 + G_4$
12	$+G_1 - G_2 - G_3 - G_4$
13	$-G_1 + G_2 - G_3 - G_4$
14	$-G_1 - G_2 + G_3 - G_4$
15	$-G_1 - G_2 - G_3 + G_4$
16	$-G_1 - G_2 - G_3 - G_4$

cross sections are averaged over the scattering angle. If  $\vec{R}_{m\gamma}^0$  (with  $\gamma=1-4$ ) stands for the positions of the protons in a tetrahedron that is centered at the origin, then

$$\langle G_\gamma G_\lambda^* + G_\gamma^* G_\lambda \rangle_{av.} = \begin{cases} 2 & \text{if } \lambda = \gamma, \\ 2f(2Q\rho/\sqrt{3}) & \text{if } \lambda \neq \gamma, \end{cases} \quad (4.13)$$

where the brackets denote an average over  $\theta_Q$  and  $\varphi_Q$ , the polar angles of  $\vec{Q}$ .  $\rho$  is the distance of the protons from the center, and

$$f(x) = \sum_{m=0}^{\infty} \frac{(-1)^m}{(2m+1)!! m!} x^{2m} \quad (4.14)$$

is a rapidly converging series in  $x$ .

From Table VIII and from Eq. (4.13) the theoretical cross sections in Table I have been calculated. The units in Table I are  $\frac{1}{24} Na_{1nc}^2 [1 - f(x)]$ , with  $x = 2\rho Q/\sqrt{3}$ . Thus the radial dependence is the same for all inelastic lines. The elastic cross section is calculated from a summation over the diagonal terms in Table VIII and over transitions between degenerate states ( $T_2 \leftrightarrow T_3$ ). One obtains  $\sigma_{e1} = \frac{1}{12} Na_{1nc}^2 [19 + 29f(x)]$ . A sum over all inelastic lines yields  $\sigma_{inel} = \frac{1}{12} Na_{1nc}^2 [29 - 29f(x)]$ . The total scattering intensity  $\sigma_{tot} = \sigma_{inel} + \sigma_{e1}$  is independent of  $Q$  and equal to  $4 Na_{1nc}^2$  as it should.

Figure 6 is a plot of the elastic and the inelastic cross sections. The point where the back scattering experiment has been performed is marked.

In  $NH_4^+ClO_4^-$  and in  $(NH_4^+)_2SnCl_6^{2-}$  the agreement between calculated scattering cross sections and the measured intensities is very good (Table I). A comparison between  $\sigma_{e1}$  and the intensity of the central component cannot be made, due to a possible contamination of the central line by Bragg

TABLE VIII.  $Q$ -dependent scattering cross section for the elastic and inelastic lines in units of  $\frac{1}{288} a_{1nc}^2$ .  $G_\gamma$  is defined in Eq. (4.11).

Transition	Levels	Cross section
1	$A-T_3$	30 $ G_3 - G_4 ^2$
2	$A-T_2$	10 $ 2G_2 - G_3 - G_4 ^2$
3	$A-T_1$	5 $ 3G_1 - G_2 - G_3 - G_4 ^2$
	$A-E$	0
4	$T_3-T_1$	6 $ G_3 - G_4 ^2$
5	$T_2-T_1$	2 $ 2G_2 - G_3 - G_4 ^2$
6	$T_3-T_2$	12 $ G_3 - G_4 ^2$
7	$T_3-E$	6 $( G_3 - G_4 ^2 + 3 G_1 - G_2 ^2)$
8	$T_2-E$	2 $( 3G_1 + G_2 - 2G_3 - 2G_4 ^2 + 3 G_3 - G_4 ^2)$
9	$T_1-E$	4 $( 2G_2 - G_3 - G_4 ^2 + 3 G_3 - G_4 ^2)$
Elastic	$A-A$	5 $ G_1 + G_2 + G_3 + G_4 ^2$
	$T_3-T_3$	36 $ G_1 + G_2 ^2$
	$T_2-T_2$	4 $ 3G_1 - G_2 + 2G_3 + 2G_4 ^2$
	$T_1-T_1$	1 $ 3G_1 - 5G_2 - 5G_3 - 5G_4 ^2$
	$E-E$	0

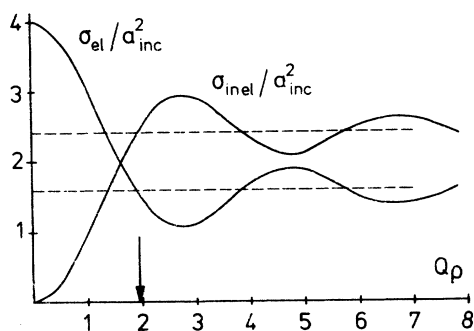


FIG. 6. Angular averages over the elastic and the inelastic scattering cross sections of the four protons in a tetrahedral group.  $\rho$  is the distance of a proton from the center of the molecule. The dashed lines give the asymptotic values of  $\sigma_{el}$  and  $\sigma_{inel}$ . The arrow denotes the value of the momentum transfer of the ammonium perchlorate experiment (Ref. 18).

peaks. In addition the incoherent scattering from nuclei other than protons also contributes to the central line.

#### V. CONCLUSIONS

In an earlier paper<sup>22</sup> a pocket state approach has been developed for the calculation of the rotational states of molecules in highly symmetric crystal fields. This formalism has now been extended to more general problems. The tunnel splitting of tetrahedral molecules in general rotational potentials has been expressed in terms of a few overlap matrix elements. Symmetry properties of the crystal field reduce the number of independent overlap matrix elements and may lead to degeneracies. The rotational wave functions have been combined with the spin-wave functions to obtain the correctly symmetrized eigenstates of a tetrahedral four-proton system.

The tunnel splitting is given by the overlap between different pocket states which depends exponentially on the potential barrier. From the usual Gruneisen parameters  $\gamma \approx 3$  one knows that the potential changes by (10–20)% when the lattice parameter is changed by 1%. A 10% variation of the potential barrier changes the tunnel

splitting by a factor 0.5 as can be seen from Fig. 5 of Ref. 22. The tunnel splitting thus is very sensitive to small changes in the potential, and pressure experiments are very well suited to obtain detailed information on the distance dependence of intermolecular forces.

$\text{NH}_4^+\text{ClO}_4^-$ , with the accidental degeneracy of two levels, is an especially challenging case. Hydrostatic pressure should lift the degeneracy and therefore three of the five lines should split into two components each. From the existing experiment one draws the conclusion that  $\Delta E(T_2, T_3)$ , the energy difference between the almost degenerate levels, is less than  $0.1 \mu\text{eV}$  (or 25 MHz). The spin symmetry of the two levels is the same; it should therefore be possible to detect the splitting by NMR methods.

The theory of neutron scattering from tunneling molecules has been developed on the basis of the pocket state formulation. For the scattering problem the pocket states have been approximated by  $\delta$  functions at the potential minima. The theory can, however, be extended (along the lines that have been used in the field of structure analysis<sup>31,32</sup>) to realistic pocket states.

The scattering from the four protons of one molecule is coherent. The angular dependence of the scattering cross section is predicted, and single-crystal experiments, to test these predictions, are suggested. Angular averages of the scattering cross section yield the radial dependence which is the same for all inelastic lines, but different for the central component. This is another prediction and it should be tested in an experiment with variable modulus of the momentum transfer and a polycrystalline sample. The relative intensities of the inelastic lines of the experiment on ammonium perchlorate and ammonium hexa-chloro-stannate are compared with the calculated scattering cross section. The agreement is very good.

#### ACKNOWLEDGMENTS

The author gratefully acknowledges many stimulating discussions with Dr. W. Press and Dr. M. Prager.

<sup>1</sup>V. Narayanamurti and R. O. Pohl, *Rev. Mod. Phys.* **42**, 201 (1970).

<sup>2</sup>E. F. Westrum and B. H. Justice, *J. Chem. Phys.* **50**, 5083 (1969).

<sup>3</sup>G. J. Vogt and K. S. Pitzer, *J. Chem. Phys.* **63**, 3667 (1975).

<sup>4</sup>K. Tomita, *Phys. Rev.* **89**, 429 (1953).

<sup>5</sup>A. Watton, A. R. Sharp, H. E. Petch, and M. M.

Pintar, *Phys. Rev. B* **5**, 4281 (1972).

<sup>6</sup>C. S. Johnson and C. Mottley, *Chem. Phys. Lett.* **22**, 430 (1973).

<sup>7</sup>W. Güttler and J. U. von Schütz, *Chem. Phys. Lett.* **20**, 133 (1973).

<sup>8</sup>J. W. Riehl, R. Wang, and H. W. Bernard, *J. Chem. Phys.* **58**, 508 (1973).

<sup>9</sup>C. A. McDowell, R. Raghunatan, and R. Srinivasan,

- Mol. Phys. 29, 815 (1975).
- <sup>10</sup>R. F. Code, J. Higinbotham, and A. R. Sharp, Can. J. Phys. 54, 239 (1976).
- <sup>11</sup>H. Glättli, A. Sentz, and M. Eisenkremer, Phys. Rev. Lett. 28, 871 (1972).
- <sup>12</sup>M. Punkkinen, J. E. Tuohi, and E. E. Ylinen, Chem. Phys. Lett. 36, 393 (1975).
- <sup>13</sup>S. Clough, T. Hobson, and S. M. Nugent, J. Phys. C 8, L95 (1975).
- <sup>14</sup>R. Windheim and H. Kinder, Phys. Lett. A 51, 475 (1975).
- <sup>15</sup>W. Press and A. Kollmar, Solid State Commun. 17, 405 (1975).
- <sup>16</sup>B. Alefeld, A. Kollmar, and B. A. Dasannacharya, J. Chem. Phys. 63, 4415 (1975).
- <sup>17</sup>M. Prager and B. Alefeld, J. Chem. Phys. 65, 4927 (1976).
- <sup>18</sup>M. Prager, B. Alefeld, and A. Heidemann, Colloque Ampère, Heidelberg (1976) (unpublished).
- <sup>19</sup>B. Alefeld and A. Kollmar, Proceedings of the Gatlinburg Conference on Neutron Research (1976) (unpublished).
- <sup>20</sup>B. Alefeld and A. Kollmar (unpublished).
- <sup>21</sup>M. Prager, W. Press, B. Alefeld, and A. Hüller (unpublished).
- <sup>22</sup>A. Hüller and D. M. Kroll, J. Chem. Phys. 63, 4495 (1975).
- <sup>23</sup>E. B. Wilson, Jr., J. Chem. Phys. 3, 276 (1935).
- <sup>24</sup>M. E. Rose, *Elementary Theory of Angular Momentum* (Wiley, New York, 1957).
- <sup>25</sup>A. Hüller and J. W. Kane, J. Chem. Phys. 61, 3599 (1974).
- <sup>26</sup>C. S. Choi, H. J. Prask, and E. Prince, J. Chem. Phys. 61, 3523 (1974).
- <sup>27</sup>A. C. Zemach and R. J. Glauber, Phys. Rev. 101, 118 (1956).
- <sup>28</sup>H. Stiller, *Inelastic Scattering of Neutrons in Solids and Liquids* (International Atomic Energy Agency, Vienna, 1963), Vol. I, p. 468.
- <sup>29</sup>S. K. Sinha and G. Venkataraman, Phys. Rev. 149, 1 (1966).
- <sup>30</sup>J. Hama and H. Miyagi, Prog. Theor. Phys. 50, 1142 (1973).
- <sup>31</sup>W. Press and A. Hüller, Acta Crystallogr. A 29, 252 (1973).
- <sup>32</sup>W. Press, Acta Crystallogr. A 29, 257 (1973).